Available online at www.sciencedirect.com
ScienceDirect
Trans. Nonferrous Met. Soc. China 24(2014) 4004−4011
Transactions of Nonferrous Metals Society of China
www.tnmsc.cn

Dielectric properties and temperature increase characteristics of zinc oxide dust from fuming furnace

Li-bo ZHANG[1,2,3,4], Ai-yuan MA[1,2,3,4], Chen-hui LIU[1,2,3,4], Wen-wen QU[1,2,3,4], Jin-hui PENG[1,2,3,4], Yong-guang LUO[1,2,3,4,5], Yong-gang ZUO[1,2,3,4]

1. Yunnan Provincial Key Laboratory of Intensification Metallurgy, Kunming 650093, China;
2. National Local Joint Laboratory of Engineering Application of Microwave Energy and Equipment Technology, Kunming 650093, China;
3. Key Laboratory of Unconventional Metallurgy of Ministry of Education, Kunming 650093, China;
4. Faculty of Metallurgical and Energy Engineering, Kunming University of Science and Technology, Kunming 650093, China;
5. Yunnan Chihong Zn & Ge Co. Ltd., Qujing 655011, China

Received 18 October 2013; accepted 14 October 2014

Abstract: Cavity perturbation method was used to determine the dielectric properties (ε', ε'', and tan δ) of zinc oxide dust in different apparent densities. The process was conducted to study the microwave-absorption properties of zinc oxide dust and the feasibility of microwave roasting zinc oxide dust to remove fluorine and chlorine. The dielectric constant, dielectric loss, and loss tangent were proportional to the apparent density of zinc oxide dust. The effects of sample mass and microwave power on the temperature increase characteristics under the microwave field were also studied. The results show that the apparent heating rate of the zinc oxide dust increases with the increase in microwave roasting power and decreases with the increase in the sample mass. The temperature of the samples reaches approximately 800 °C after microwave treatment for 8 min, which indicates that the zinc oxide dust has strong microwave-absorption ability.

Key words: zinc oxide dust; apparent density; dielectric properties; microwave heating; temperature increase characteristics

1 Introduction

Zinc is an important metal that is used in the metallurgical, chemical, and textile industries. It is extracted mainly from sulfide ore. A part of zinc is recycled from zinc-containing wastes such as zinc dust, zinc ash, and zinc dross. The zinc industry is developing rapidly but its operations are constrained by limited resources, energy shortages, and ecological and environmental problems [1−3]. A large amount of zinc oxide dusts are produced during the smelting of zinc, lead, and copper, as well as the scrap recycling process of galvanized steel. Zinc oxide dust has significant recovery and profit margin because of the high content of valuable Zn, Pb and In [4−6]. Zinc oxide dust obtained from a lead fuming furnace also contains a large number of fluorine and chlorine impurities during the zinc hydrometallurgy process; this condition results in equipment corrosion, high production costs, and low zinc recovery [7,8]. Thus, finding an effective method to solve these problems and reuse the secondary resource is necessary [9−11]. Currently, two main methods in fluorine and chlorine removal from zinc oxide dust are adopted: pretreatment removal and leach liquor removal [12,13]. However, both methods involve high energy consumption and management difficulties in the subsequent process. The microwave removal method is considered an environmentally friendly and energy-saving alternative.

As an efficient and clean form of energy, microwave heating has been widely used in mineral processing and metallurgy. Compared with conventional heating, microwave heating has the following advantages: fast

Foundation item: Project (51104073) supported by the National Natural Science Foundation of China; Project (2014CB643404) supported by the National Basic Research Program of China; Project (2013AA064003) supported by the Hi-tech Research and Development Program of China; Project (2012HB008) supported by the Yunnan Provincial Young Academic Technology Leader Reserve Talents, China
Corresponding author: Jin-hui PENG; Tel: +86-871-5191046; Fax: +86-871-5138997; E-mail: jhpeng@kmust.edu.cn
DOI: 10.1016/S1003-6326(14)63562-7

heating rate, volume heating, selective heating, easy automatic control, and the absence of environmental pollution. It can also reduce the reaction temperature, shorten the reaction time, and promote energy conservation [14−20]. With these advantages, microwave heating is introduced to remove fluorine and chlorine from zinc oxide dust. Microwave heating is employed in the microwave field dielectric loss of metallurgical material to ensure the overall heating of the material. The heating is determined by the material dielectric parameters (complex permittivity), which are key physical parameters to describe the interaction mechanism between microwave and dielectric materials. However, microwave heating is selective with regard to materials of different dielectric properties. Microwave selectively heats high-loss substances and low-loss substances that have no obvious absorption [21−24].

The dielectric properties (ε', ε'', and $\tan\delta$) of material are employed to describe the microwave absorption characteristics in the microwave heating process [25−28]. Dielectric properties can be defined in terms of relative permittivity (ε) composed of a real part (ε') and an imaginary part (ε''). The real part of the relative permittivity is known as dielectric constant and the imaginary part as loss factor. These properties can be expressed using the equation of $\varepsilon=\varepsilon'-j\varepsilon''$.

Loss tangent ($\tan\delta$) is a parameter employed to describe how well a material absorbs microwave energy. It represents the ratio of the dielectric loss factor to the dielectric constant ($\tan\delta=\varepsilon''/\varepsilon'$). The dielectric constant and loss tangent are functions of measurement frequency, material homogeneity and anisotropy, moisture, and material temperature.

The effects of various factors, such as microwave frequency, relative density and particle size of powder samples, on the permittivity and permeability were investigated. The ε' values of powders SiO_2 and Fe_3O_4 with the relative density below 1 are smaller than those estimated by the linear relation between ε' and the relative density, and larger than those estimated by the Lichtenecker's logarithm mixed law [29].

In this study, the cavity perturbation method was adopted to measure the dielectric properties of zinc oxide dust with different apparent densities. The zinc oxide dust temperature increase characteristics through microwave heating was also investigated to provide a theoretical basis for the removal of fluorine and chlorine from zinc oxide dust.

2 Experimental

2.1 Experimental materials

The zinc oxide dust used in this study was obtained from a lead and zinc smelting plant in Yunnan province, China. The main chemical composition of the zinc oxide dust sample is shown in Table 1, and its XRD pattern is presented in Fig. 1.

Table 1 Chemical composition of zinc oxide dust sample (mass fraction, %)

Zn	Pb	Ge	Cd	Fe	Sb
53.17	22.38	0.048	0.21	0.38	0.23
S	As	F	Cl	SiO_2	CaO
3.84	1.04	0.0874	0.0783	0.65	0.096

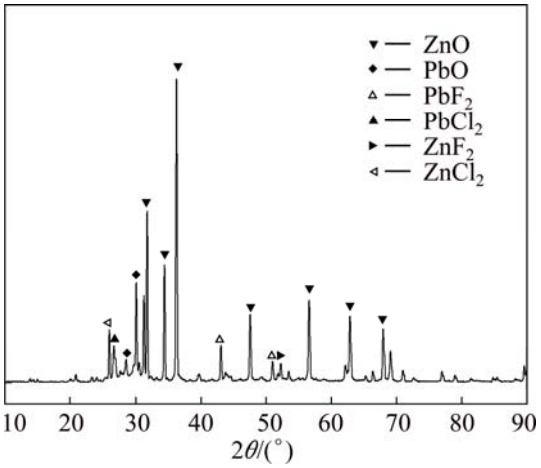

Fig. 1 XRD pattern of zinc oxide dust sample

As shown in Table 1 and Fig. 1, the zinc oxide dust sample contained a significant amount of lead and zinc, mainly in the form of lead and zinc oxides. Figure 2 shows three different morphologies of zinc oxide dust: cubic crystal structure, floc structure, and spherical structure. Zn mainly existed in the ZnO phase; Pb mainly existed in the PbO phases; while F and Cl mainly existed in zinc and lead halide. Certain amounts of fluorine and chlorine compounds were also found. The fluorine and chlorine compounds were dissolved in leaching solution during the leaching process. The excess content of fluorine and chlorine elements resulted in equipment corrosion, high production costs, and low zinc recovery in the subsequent zinc electrolysis process. Microwave was directly applied to roasting the zinc oxide fumes according to the different microwave absorbances among halides, lead, and zinc oxides in combination with the advantages of selective microwave heating, for the purpose of strengthening the separation of halides as volatile components.

2.2 Microwave heating system to measure temperature increase characteristics

The experiment equipment included a 3 kW box-type microwave metallurgical reactor developed by the Key Laboratory of Unconventional Metallurgy,

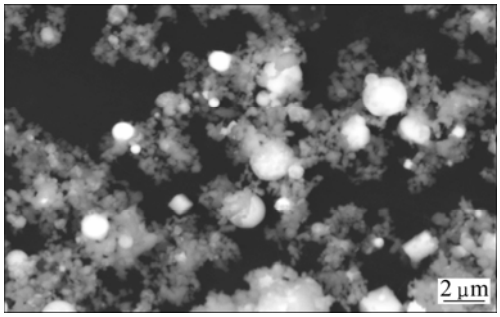

Fig. 2 SEM image of zinc oxide dust sample

Kunming University of Science and Technology, China. A schematic diagram of the microwave heating system is shown in Fig. 3.

The microwave device had automatic temperature control with microwave heating frequency of 2450 MHz and continuous adjustable power of 0−3 kW. A thermocouple with a shielded sleeve was used to measure the temperature of the samples, which ranged from 0 to 1300 °C. The zinc oxide dust samples were placed in a mullite crucible with an inner diameter of 90 mm and a height of 120 mm. Thereafter, the samples were placed into the microwave cavity resonator sensor. The mullite crucible showed good properties, such as wave transparency and heat shock resistance. The smoke soot absorption system was composed of a dust collection bottle, two water bottles, an alkali absorption bottle, a buffer bottle, and a miniature pump. This system was able to collect and absorb the flue gas and flue dust generated during the experimental process.

2.3 Test principle of dielectric characteristics and system

2.3.1 Cavity perturbation test principle

The resonant cavity perturbation method [30] has been widely adopted because of its high measurement accuracy and wide sphere of application. The dielectric property measurement method is based on the cavity perturbation method that employs a single resonant mode. The change in the cavity characteristics in the presence of a sample has been measured. Based on a sample in the resonant cavity, the principles can be expressed as follows [31]:

$$\frac{\Delta\omega}{\omega}=-\omega_0(\varepsilon_r'-1)\int_{V_e}E_0^*E\mathrm{d}v/(4W) \tag{1}$$

$$\frac{1}{Q}-\frac{1}{Q_0}=2\varepsilon_0\varepsilon'\int_{V_e}E_0^*E\mathrm{d}v/(4W) \tag{2}$$

$$W=\int_V(E_0^*D_0+H_0^*B_0)+(E_0^*D_1+H_0^*B_1)\mathrm{d}v \tag{3}$$

where $\Delta\omega=\omega-\omega_0$, $\Delta\omega$ is the angular frequency deviation; ω_0 is the resonance frequency of the cavity in the unperturbed condition; ω represents the corresponding parameters of the cavity loaded with the sample; ε_r' and ε_r'' are the real and imaginary parts of the complex permittivity of the sample, respectively; V and V_e are the volumes of the cavity and the sample, respectively; E_0^*, D_0, H_0^*, and B_0 are the interior fields of the sample; E is the field strength of the cavity; dv is the elemental volume; Q_0 is the resonance frequency of the cavity in the unperturbed condition; Q represents the corresponding parameter of the cavity loaded with the sample; W is the storage energy; D_1 and B_1 are the added values of the electric displacement and magnetic induction intensity, respectively.

The measurement principle of the cavity perturbation is illustrated in Fig. 4. Both the reflection coefficient and resonant frequency were recorded by the microwave sensor connected to the software. The dielectric constant and loss factor were calculated based

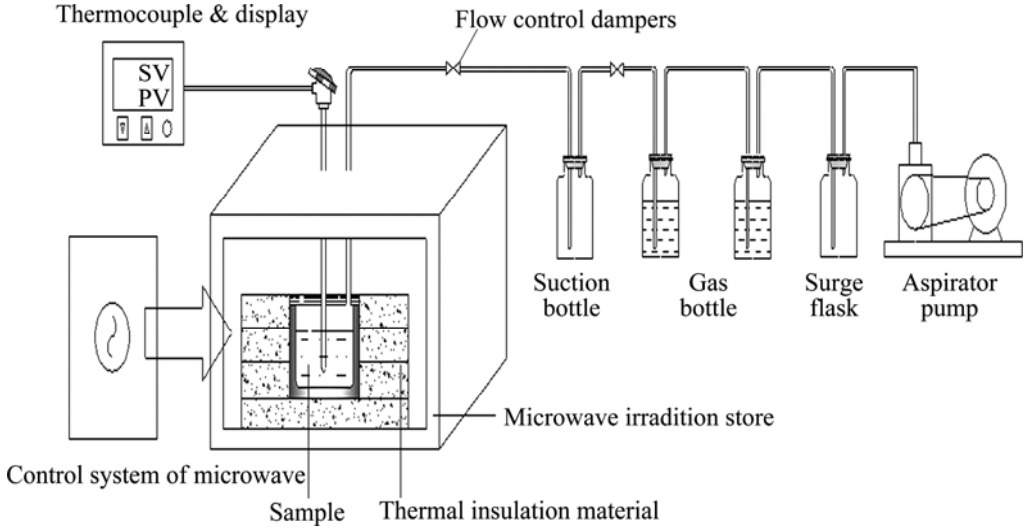

Fig. 3 Schematic diagram of microwave heating system

on the reflection coefficient and resonance frequency variation under the empty sensor and filled with the sample, respectively.

2.3.2 Test equipment and process

The dielectric parameter measuring device for zinc oxide dust is shown in Fig. 5. The dielectric property testing equipment was a dielectric parameter tester (dielectric kit for vials). The device consisted of a microwave power source, a microwave receiver, and a cavity resonator. The microwave signal receiver of AD−8320 integrated circuit could detect the signal amplitude and phase. A resonator was also used in the cavity. A test control unit was connected to the computer test software via a USB data cable. A test sample was first placed in a small bottle with almost the same size as the cavity resonator. The bottle was placed into the cavity resonator through the opening holes. The dielectric parameters could be calculated with the cavity perturbation theory by comparing the resonance frequency and quality factor before and after the test.

The dried zinc oxide dust was divided into 11 parts that were weighed and placed in sealed quartz standard tubes of known volume at (21±1) °C and frequency of 2.45 GHz. Each sample was subsequently pressed to obtain 11 different densities. The apparent density of the zinc oxide dust was calculated using the sample mass and volume in the standard pipe. The system error on the real part of the dielectric coefficient was controlled at 3%−5% [26] during the perturbation method tests. With deionized water (the real part of the dielectric constant was 78) and polytetrafluoroethylene (the real part of the dielectric coefficient was 2.08) as standards, results were 76.79 and 2.04, respectively. The real and measured values had differences of 1.55% and 1.92%, respectively, which indicate that the measurement results of small volume perturbation were credible by the perturbation method.

3 Results and discussion

3.1 Dielectric properties of zinc oxide dust

The measured material of the dielectric properties is related to a number of factors, such as density, humidity, and frequency. This study mainly discusses the effect of apparent density on the dielectric properties of zinc oxide dust.

3.1.1 Effect of apparent density on dielectric properties

The effects of apparent density on the dielectric constant, dielectric loss, and loss tangent are presented in Figs. 6(a)−(c), respectively.

As shown in Fig. 6, the dielectric properties (ε', ε'', and $\tan\delta$) of the zinc oxide dust have a good linear relationship with the apparent density. Table 2 shows the linear regression equation and the correlation coefficient (R^2).

Figure 6 shows that apparent density is small (<2.8 g/cm^3), dielectric constant (ε'), loss factor (ε'') and loss tangent ($\tan\delta$) stay at a relatively low level and the change trend is not obvious. Because the zinc oxide dust apparent density is relatively small, standard tube

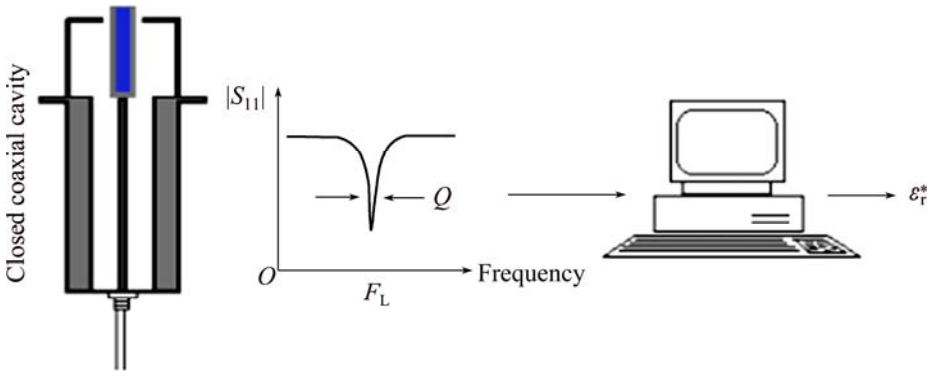

Fig. 4 Schematic diagram of measurement principle of cavity perturbation

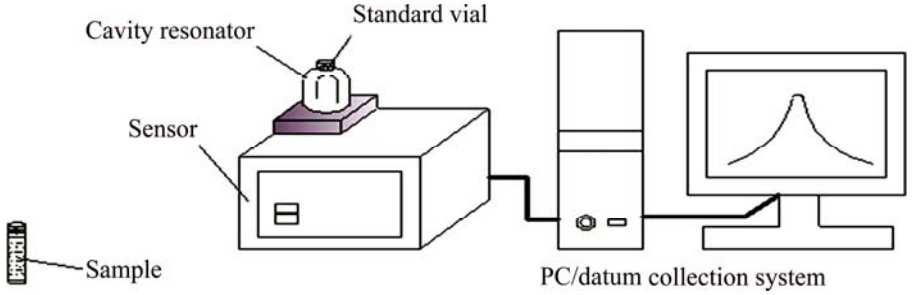

Fig. 5 Schematic diagram of zinc oxide dust dielectric constant measurement device

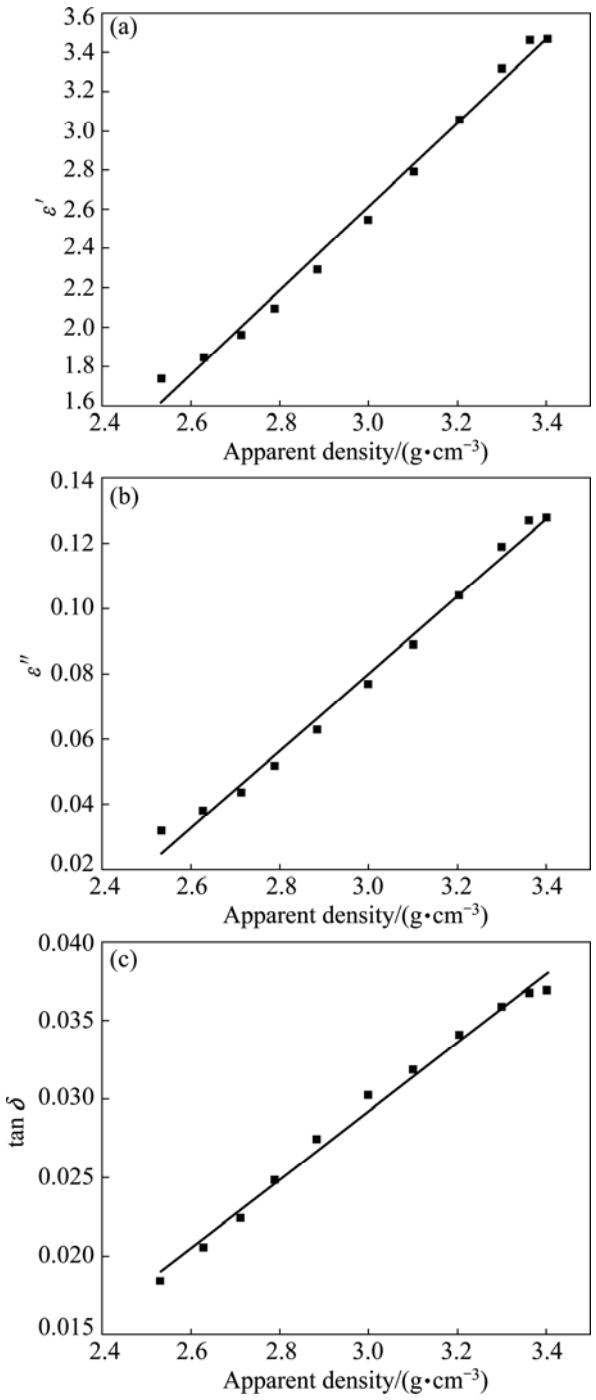

Fig. 6 Effect of apparent density on dielectric constant ε' (a), loss factor ε'' (b) and loss tangent tan δ (c)

for testing has a large number of voids between material particles full of air. And with the increase of apparent density, the air which is between material particles is continuous discharge, and dielectric characteristics values of zinc oxide dust (ε', ε'') change significantly.

When the apparent density is low (<3.2 g/cm^3), the value of the dielectric properties (ε', ε'' and tan δ) increases linearly with the apparent density. Thus, the change trend is not obvious. The increase in the apparent density increases the dielectric properties, thereby increasing the microwave absorption ability. More heat energy converted from microwave energy may be the reason for the increase in the dielectric properties.

3.1.2 Apparent density effect on microwave penetration depth

The microwave penetration depth (D_p) was measured as the distance from the surface to the inner part of the material, where the microwave field intensity was reduced to 1/e of the original field intensity. This value can be expressed as follows [32−34]:

$$D_p = \frac{\lambda_0}{2\sqrt{2\pi}\sqrt{\varepsilon'\left[1+\left(\frac{\varepsilon''}{\varepsilon'}\right)^2-1\right]}} \quad (4)$$

In Eq. (4), D_p determines the microwave heating uniformity of the material at 2.45 GHz and λ_0=12.24 cm.

The microwave penetration depth of the zinc oxide dust was calculated at different apparent densities. The effect of apparent density on the microwave penetration depth is illustrated in Fig. 7. The results show that D_p decreases when the apparent density increases. Based on the curves and the regression equations reported in Table 2, with the increase in the apparent density, the material absorbed more microwave energy. The energy was converted into heat along with the decay of the microwave field strength and power, which determined the microwave penetration depth. This result is consistent with the conclusion presented by PENG and YANG [22]. When the material penetration depth was greater than the size of the heated sample, the influence was negligible. By contrast, the microwave energy penetration was limited when the sample size was larger than the penetration depth. Non-uniformly heating also occurred during the microwave heating. Thus, the suitable apparent density was essential to fully employ the volumetric microwave heating process.

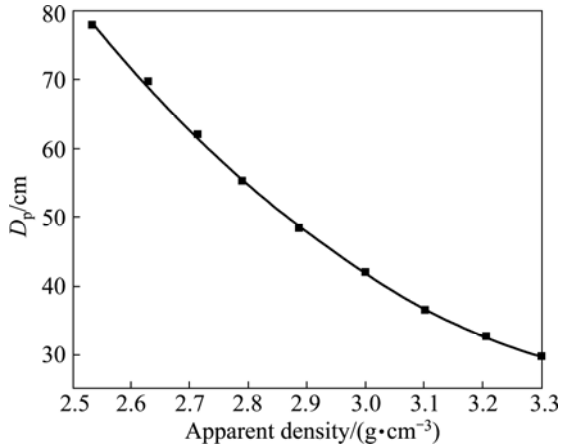

Fig. 7 Effect of apparent density on microwave penetration depth

Table 2 Regression equations on zinc oxide dust material dielectric property in different densities (x: apparent density)

Item	Linear regression equation	R^2
ε'	ε'=2.14119x−3.81184	0.9892
ε''	ε''=0.11806x−0.27402	0.98927
tan δ	tan δ=0.02186x−0.03641	0.98909
D_p	D_p=49.8097x^2−353.8286x+655.0319	0.99934

3.2 Microwave heating characteristics of zinc oxide dust

3.2.1 Effect of sample mass on temperature increase characteristics

The temperature increase characteristics and the sample mass in the microwave field are closely related to each other. In the microwave field, the sample mass of the zinc oxide dust affects the heating behavior under a microwave power setting of 900 W, as shown in Fig. 8.

The relationship between the temperature (T_m) of the zinc oxide dust and time for samples with different masses of 100, 200, and 300 g is illustrated in Fig. 8. The empirical equations are shown in Eqs. (5)−(7):

$$T_m=54.45517.309t+28.073t^2-1.635t^3,\ R^2=0.9950 \quad (5)$$

$$T_m=66.28940.393t+20.787t^2-0.923t^3,\ R^2=0.9942 \quad (6)$$

$$T_m=62.58633.955t+13.119t^2-0.465t^3,\ R^2=0.9960 \quad (7)$$

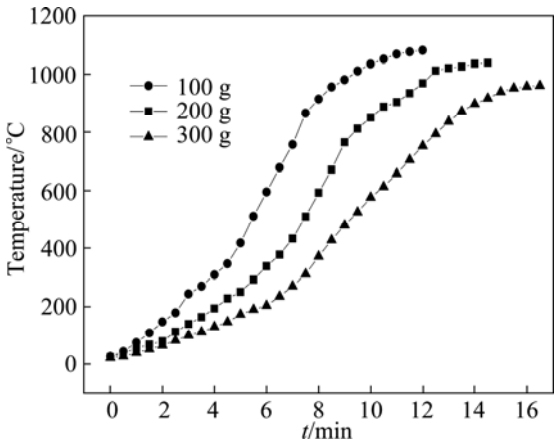

Fig. 8 Heating rate curves of zinc oxide dust with different masses in microwave field

The results show that the average heating rates of zinc oxide fume were 90, 72, and 58 °C/min, respectively. Thus, a smaller mass of sample indicates a faster apparent heating rate.

In the microwave field, the effect of the sample mass of zinc dust on the heating rate can be calculated as follows [35]:

$$\frac{\mathrm{d}T}{\mathrm{d}\tau}=\frac{T-T_0}{\tau}=\frac{2\pi f\varepsilon_0\varepsilon''E^2}{\rho Vc_p}=\frac{2\pi f\varepsilon_0\varepsilon''E^2}{mc_p} \quad (8)$$

where T is the material heating temperature; T_0 is the material initial temperature; τ is the time; m is the mass of material; c_p is the specific heat capacity of material; f is the frequency of the microwave; ε_0 is the vacuum permittivity; ε'' is the dielectric loss factor; E is the electric field strength.

As shown in Eq. (8), the greater the dust mass is, the smaller the heating rate is. This observation is in accordance with the experimental results. On one hand, the sample mass of the materials increased as the microwave power density per unit mass of sample decreased. The increasing sample mass also increased the contact areas of the sample and resulted in increasing heat dissipation to the external environment. On the other hand, when microwave power was constant, a larger amount of zinc oxide dust indicated a thicker sample and the need for more microwave power. In the experimental condition range, the power density of the sample decreased with the increase in the sample mass, which resulted in a slower rate of temperature increase.

3.2.2 Effect of microwave power on temperature increase characteristics

The heating curves of 300 g zinc oxide dust at microwave powers of 900, 1200 and 1800 W are presented in Fig. 9. The empirical formulas of T_m and time are shown in Eqs. (9)−(11):

$$T_m=62.58633.955t+13.119t^2-0.465t^3,\ R^2=0.9960 \quad (9)$$

$$T_m=65.37037.373t+19.040t^2-0.813t^3,\ R^2=0.9963 \quad (10)$$

$$T_m=48.63211.821t+26.286t^2-1.519t^3,\ R^2=0.9965 \quad (11)$$

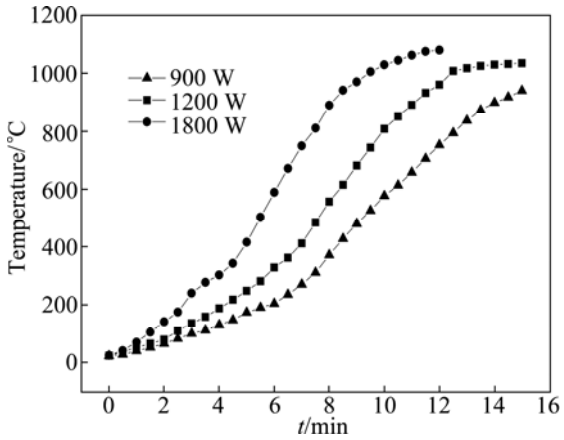

Fig. 9 Heating rate curves of zinc oxide dust at different microwave powers

As illustrated in Fig. 9, microwave power has obvious effects on the temperature increase rate under the same conditions. The microwave power increased the apparent average heating rate of zinc oxide dust, and higher microwave power required shorter heating time to reach the same temperature. The experimental result is similar to the reported results for microwave heating of

low-grade nickel oxide ore [36]. The reason for this observation is that the temperature of the material increases with the increasing microwave output power within a certain range.

The per unit volume of the zinc oxide dust also absorbed microwave power or the microwave energy dissipated power in the dust. This value can be expressed as [37]

$$P=2\pi f\varepsilon''E^2 \quad (12)$$

where f is the microwave frequency; E is the electric field strength.

In Eq. (12), the increasing microwave power indicated that the increasing electric field strength in other conditions was unchanged. Microwaves could penetrate the interior of the material and would result in heating uniformity. The zinc oxide dust absorbed more microwave energy with the increase in E, which resulted in temperature increase. Therefore, increasing the microwave heating power properly could reduce the heating time and improve the apparent average heating rate of the zinc oxide dust.

In the process of roasting, microwave heating took full advantage of dielectric loss of the zinc oxide dust and selectively heat molecules or atoms which have good microwave absorbance. The zinc oxide dust in microwave field reaches 800 °C within 8 min, which provides a well thermodynamic condition for defluorination and dechlorination by microwave roasting. The microwave absorbance of chloride and sulfide is strong, while that of Zn or Pb oxide is weak in the zinc oxide fume. Capitalizing on the selective heating property of microwaves can strengthen the separation of fluorides and chlorides in volatile components. The successful outcome of this research will provide the theoretical basis for effectively separating fluorine and chlorine as well as efficiently producing zinc with low energy consumption from the zinc oxide dust.

4 Conclusions

1) The dielectric properties (ε', ε'' and tan δ) of zinc oxide dust have a good linear relationship with the apparent density. The dielectric properties increase when the apparent density increases. The microwave penetration depth decreases when the apparent density increases.

2) The material heating rate is affected by the sample mass at the output power of 900 W in the microwave field. As the zinc oxide dust mass increases, the heating rate slows down. When mass is kept constant, the temperature increase rate of zinc oxide dust is affected by the microwave power. Increasing the microwave heating power appropriately could reduce the heating time and improve the apparent average heating rate of the zinc oxide dust.

3) Zinc oxide dust has good absorption properties and can be heated quickly in the microwave field. This condition provides a theory to remove fluorine and chlorine at 800 °C in 8 min by microwave, which can provide a clean and energy-efficient method to treat zinc-containing wastes. The results can also provide a theoretical basis for exploring new technology to remove fluorine and chlorine in zinc oxide dust.

References

[1] MA Hua-ju, HE Hang-jun, LI Hao-ming. Comprehensive utilization of restoring volatilizable secondary zinc oxide [J]. Nonferrous Metals, 2010(4): 16−17, 28. (in Chinese)

[2] LI Yu-hu, LIU Zhi-hong, ZHAO Zhong-wei, LI Qi-hou, LIU Zhi-yong, ZENG Li. Determination of arsenic speciation in secondary zinc oxide and arsenic leachability [J]. Transactions of Nonferrous Metals Society of China, 2012, 22(5): 1209−1216.

[3] RUIZ O, CLEMENTE C, ALONSO M, ALGUACIL F J. Recycling of an electric arc furnace flue dust to obtain high grade ZnO [J]. Journal of Hazardous Materials, 2007, 141(1): 33−36.

[4] LIU Qing, YANG Sheng-hai, CHEN Yong-ming, HE Jing, XUE Hao-tian. Selective recovery of lead from zinc oxide dust with alkaline Na_2EDTA solution [J]. Transactions of Nonferrous Metals Society of China, 2014, 24(4): 1179−1186.

[5] LI Xuan-hai, ZHANG Yan-juan, QIN Quan-lun, YANG Jian, WEI Yan-song. Indium recovery from zinc oxide flue dust by oxidative pressure leaching [J]. Transactions of Nonferrous Metals Society of China, 2010, 20(S1): s141−s145.

[6] PENG J, PENG B, YU D, TANG M T, LOBEL J, KOZINSKI J A. Volatilization of zinc and lead in direct recycling of stainless steel making dust [J]. Transactions of Nonferrous Metals Society of China, 2004, 14(2): 392−396.

[7] RESIN N G, TOPKAYA Y A. Dechlorination of a zinc dross [J]. Hydrometallurgy, 1998, 49(1−2): 179−187.

[8] ŞAHIN F Ç, DERIN B, YÜCEL O. Chloride removal from zinc ash [J]. Scandinavian Journal of Metallurgy, 2000, 29(5): 224−230.

[9] MA Hua-ju, SHI Wen-ge, ZHENG Yan-qiong. Research on a new technology of producing electrolytic zinc by complex-componential sub-zinc oxide [J]. Journal of Non-ferrous Metallurgy, 2010(3): 52−55. (in Chinese)

[10] LI Dong, WANG Jian-hua, GUO Xiao-hui, HU Yuan-ming. Practical study on producing electrolytic zinc from secondary zinc oxide [J]. Non-ferrous Mining and Metallurgy, 2011, 27(3): 33−37. (in Chinese)

[11] JHA M K, KUMAR V, SINGH R J. Review of hydrometallurgical recovery of zinc from industrial wastes[J]. Resources Conservation and Recycling, 2001, 33(1): 1−22.

[12] MASON C R S, HARLAMOVS J R, DREISINGER D B, GRINBAUM B. Solvent extraction of a halide from a aqueous sulphate solution: US, 7037482 B2[P]. 2006.

[13] BODSON F J J. Process for the elimination of chloride from zinc sulphate solution: US, 4005174[P]. 1977−01−25.

[14] JIN Qin-han, DAI Shu-san, HUANG Ka-ma. Microwave chemistry [M]. Beijing: Science Press, 1999. (in Chinese)

[15] TONG Zhi-fang, BI Shi-wen, YANG Yi-hong. Present situation of study on microwave heating application in metallurgy [J]. Journal of Materials and Metallurgy, 2004, 3(2): 117−120. (in Chinese)

[16] CAI Wei-quan, LI Hui-quan, ZHANG Yi. Recent development of microwave radiation application in metallurgical processes [J]. The

Chinese Journal of Process Engineering, 2005, 5(2): 228−232. (in Chinese)
[17] ZHENG Ying, NIU Yu-qing, NIU Xue-jun, WU Pei-sheng. The application of microwave for processing minerals [J]. Uranium Mining and Metallurgy, 2002, 21(3): 151−153. (in Chinese)
[18] KINGMAN S W, ROWSON N A. Microwave treatment of minerals—A review [J]. Minerals Engineering, 1998, 11(11): 1081−1087.
[19] HAQUE K E. Microwave energy for mineral treatment processes—A brief review [J]. International Journal of Mineral Processing, 1999, 57(1): 1−24.
[20] BAO R, YI J H, PENG Y D, ZHANG H Z. Effects of microwave sintering temperature and soaking time on microstructure of WC−8Co [J]. Transactions of Nonferrous Metals Society of China, 2013, 23(2): 372−376.
[21] BERGESE P. Specific heat, polarization and heat conduction in microwave heating systems: A nonequilibrium thermodynamic point of view [J]. Acta Materialia, 2006, 54(7): 1843−1849.
[22] PENG Jin-hui, YANG Xian-wan. The new applications of microwave power [M]. Kunming: Yunnan Science and Technology Press, 1997. (in Chinese)
[23] METAXAS A C, MEREDITH R J. Industrial microwave heating [M]. London: Peter Peregrinus, 1983.
[24] CLARK D E, FOLZ D C, WEST J K. Processing materials with microwave energy [J]. Materials Science and Engineering A, 2000, 287(2): 153−158.
[25] LIN Wei-gan. Microwave theory and technology [M]. Beijing: Science Press, 1979. (in Chinese)
[26] DONG Shu-yi. Microwave measuring [M]. Beijing: Beijing University of Science and Technology Press, 1991. (in Chinese)
[27] BÜYÜKÖZTÜRK O, YU T Y, ORTEGA J A. A methodology for determining complex permittivity of construction materials based on transmission-only coherent, wide-bandwidth free-space measurements [J]. Cement and Concrete Composites, 2006, 28(4): 349−359.
[28] DING D H, ZHOU W C, LUO F, ZHU D M. Influence of pyrolytic carbon coatings on complex permittivity and microwave absorbing properties of Al_2O_3 fiber woven fabrics [J]. Transactions of Nonferrous Metals Society of China, 2012, 22(2): 354−359.
[29] HOTTA M, HAYASHI M, NISHIKATA A, NAGATA K. Complex permittivity and permeability of SiO_2 and Fe_3O_4 powders in microwave frequency range between 0.2 and 13.5 GHz [J]. ISIJ International, 2009, 49(9): 1443−1448.
[30] HUANG Ming, PENG Jin-Hui, ZHANG Shi-min, ZHANG Li-bo, XIA Hong-ying, YANG Jing-jing. Measuring methods of the material permittivity and it's applications [C]//The 12th National Microwave Can Application Academic Conference Proceedings. Chengdu: China Microwave Society, 2005: 79−91.
[31] CARTER R G. Accuracy of microwave cavity perturbation measurements [J]. IEEE Transaction on Microwave Theory and Techniques, 2001, 49(5): 918−923.
[32] GUO W C, WANG S J, GOPAL T, JUDY A J, TANG J M. Temperature and moisture dependent dielectric properties of legume flour associated with dielectric heating [J]. LWT - Food Science and Technology, 2010, 43(2): 196−201.
[33] KUMAR P, CORONEL P, SIMUNOVIC J, TRUONG V D, SANDEEP K P. Measurement of dielectric properties of pumpable food materials under static and continuous flow conditions [J]. Journal of Food Science, 2007, 72(4): E177−E183.
[34] PENG Z W, HWANG J Y, MOURIS J, HUTCHEON R, HUANG X D. Microwave penetration depth in materials with non-zero magnetic susceptibility [J]. ISIJ International, 2010, 50(11): 1590−1596.
[35] CHEN Jin, LIN Wan-ming, ZHAO Jing. The coking coal metallurgy technology [M]. Beijing: Chemical Industry Press, 2007. (in Chinese)
[36] HUA Yi-xin, TAN Chun-e, XIE Ai-jun, LV Hong. Microwave-aided chloridizing of nickel-bearing garnierite ore with $FeCl_3$ [J]. Nonferrous Metals, 2000, 52(1): 59−60. (in Chinese)
[37] THOSTENSON E T, CHOU T W. Microwave processing: fundamentals and applications [J]. Composites, Part A: Applied Science and Manufacturing, 1999, 30(9): 1055−1071.

烟化炉产氧化锌烟尘的介电特性及温升特性

张利波[1,2,3,4]，马爱元[1,2,3,4]，刘晨辉[1,2,3,4]，曲雯雯[1,2,3,4]，彭金辉[1,2,3,4]，罗永光[1,2,3,4,5]，左勇刚[1,2,3,4]

1. 云南省特种冶金重点实验室，昆明 650093；
2. 微波能工程应用及装备技术国家地方联合工程实验室，昆明 650093；
3. 非常规冶金教育部重点实验室，昆明 650093；
4. 昆明理工大学 冶金与能源工程学院，昆明 650093；
5. 云南驰宏锌锗股份有限公司，曲靖 655011

摘　要：为了研究微波焙烧脱除氧化锌烟尘中氟氯的可行性以及氧化锌烟尘的吸波特性，采用谐振腔微扰法对不同物料密度氧化锌烟尘的介电特性(ε', ε'' 和 tan δ)进行测定。氧化锌烟尘的介电常数、介电损耗和损耗角正切值与氧化锌烟尘的表观密度成正比。在微波场下研究物料质量和微波功率对氧化锌烟尘升温特性的影响。结果表明，氧化锌烟尘对微波具有较强的吸波能力，其表观升温速率与微波焙烧功率成正比，与质量成反比，在 8 min 内温度可到达 800 ℃。

关键词：氧化锌烟尘；表观密度；介电特性；微波加热；温升特性

(Edited by Xiang-qun LI)